

Supporting Information

In-situ Generation of CoS_{1.097} Nanoparticles on S/N Co-Doped Graphene/Carbonized Foam for Mechanically Tough and Flexible All Solid-State Supercapacitors

Degang Jiang,^{†ab} Hui Liang,^{†b} Yan Liu,^b Yiwei Zheng,^b Chenwei Li,^{*b} Wenrong Yang,^{*c} Colin J. Barrow^c and Jingquan Liu^{*ab}

^a College of Materials Science and Engineering, Linyi University, Linyi 276005, China

^b College of Materials Science and Engineering, Institute for Graphene Applied Technology Innovation, Qingdao University, Ningxia Road 308 Qingdao 266071, China.

E-mail: jliu@qdu.edu.cn (Jingquan Liu) and lichenwei@qdu.edu.cn (Chenwei Li)

^c School of Life and Environmental Sciences, Deakin University, VIC 3217, Australia.

E-mail: wenrong.yang@deakin.edu.au (Wenrong Yang)

[†] Degang Jiang and Hui Liang contributed equally to this work.

Characterizations

TEM image was obtained on a JEM-2100F electron microscope with an accelerating voltage of 200 kV. The morphology and structure of the as-prepared samples were investigated by JEOL 6701 field-emission scanning electron microscope (JEOL 6701, Japan) and energy dispersive X-ray spectroscopy. The XPS spectra of as-prepared samples were examined on a PerkinElmer PHI-5702 multifunctional X-ray photoelectron spectroscope (XPS, Physical Electronics, USA). The structures of the as-prepared samples were analyzed with XRD (DX2700, China) at a scan rate (2θ) of 2° min^{-1} ranging from 5° to 80° , operating at Cu K α radiation ($\lambda=1.5418 \text{ \AA}$) with an accelerating voltage of 40 kV and an applied current of 30 mA. The mechanical properties of composite films and supercapacitor devices were measured by using a Dynamic Mechanical Analyzer (TAG92-DMA Q800), and all the samples were tested at room temperature. All the electrochemical tests were performed using a CHI 760E electrochemical workstation.

Calculations

The electrochemical properties of the CoS_{1.097}/GF composite and the control

electrodes were measured using a three-electrode system in a 6 M KOH aqueous solution. The prepared samples were used as the working electrodes, Pt foil as the counter electrode, and Hg/HgO electrode as the reference electrode, respectively. The specific capacitances of the CoS_{1.097}/GF composite and the control electrodes were calculated from their galvanostatic charge/discharge (GCD) curves according to the following equation:

$$C = \frac{I\Delta t}{m\Delta V} \quad (1)$$

Where C is the specific capacitance (F g⁻¹), I is the discharge current (A), Δt is the discharge time (s), m (g) is the total mass of the working electrode and ΔV is the voltage window (V).

The CoS_{1.097}/GF||GF a-EC devices were measured in a two-electrode configuration. The specific capacitances of the CoS_{1.097}/GF||GF a-EC devices were calculated from their galvanostatic charge/discharge (GCD) curves according to the following equation:

$$C = \frac{I\Delta t}{m\Delta V} \quad (2)$$

Where C is the specific capacitance (F g⁻¹), I is the discharge current (A), Δt is the discharge time (s), m (g) is the total mass of the anode and cathode electrodes and ΔV is the voltage window (V).

The energy density and power density of symmetrical supercapacitor systems were calculated using the following equations:

$$E = \frac{C_t \Delta V^2}{2 \times 3.6}$$

$$P = \frac{E}{t} \quad (3)$$

$$(4)$$

Where E (Wh kg⁻¹) is the energy density, P (W kg⁻¹) is the power density of the

CoS_{1.097}/GF||GF a-EC devices, C_t (F g⁻¹) is the specific capacitance of the whole the CoS_{1.097}/GF||GF a-EC devices, which is equal to $C/2$. ΔV (V) is the voltage window, and t (h) is the discharge time, respectively.

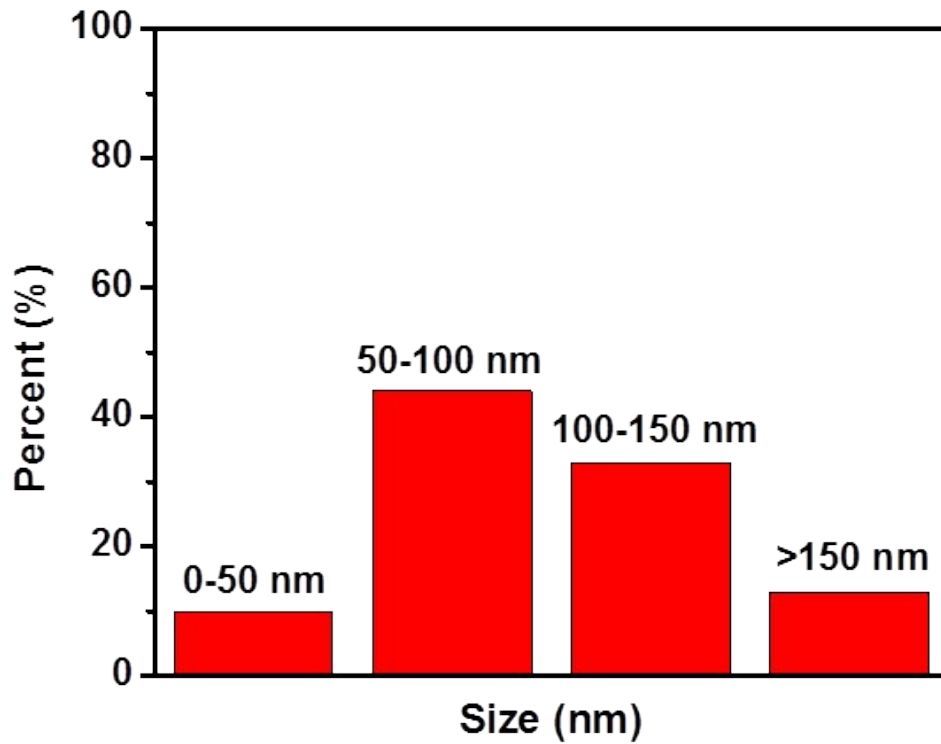


Fig. S1 The size distribution of the CoS_{1.097} NPs on S/N co-doped RGO sheets.

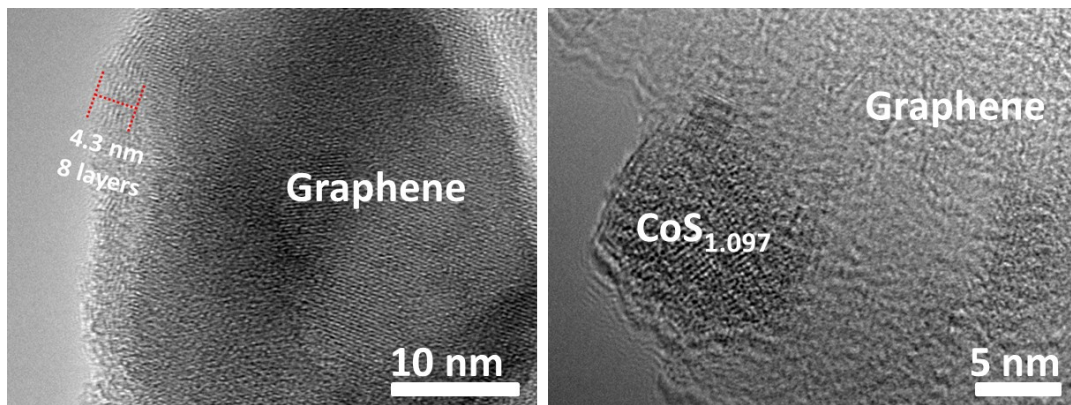


Fig. S2 HRTEM images of S/N co-doped RGO sheets.

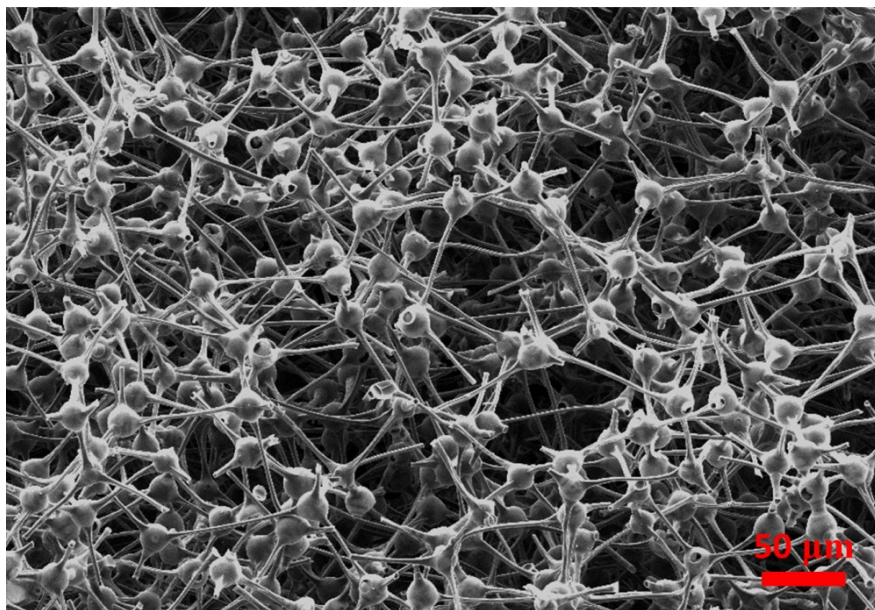


Fig. S3 SEM image of the carbonized MF (CMF).

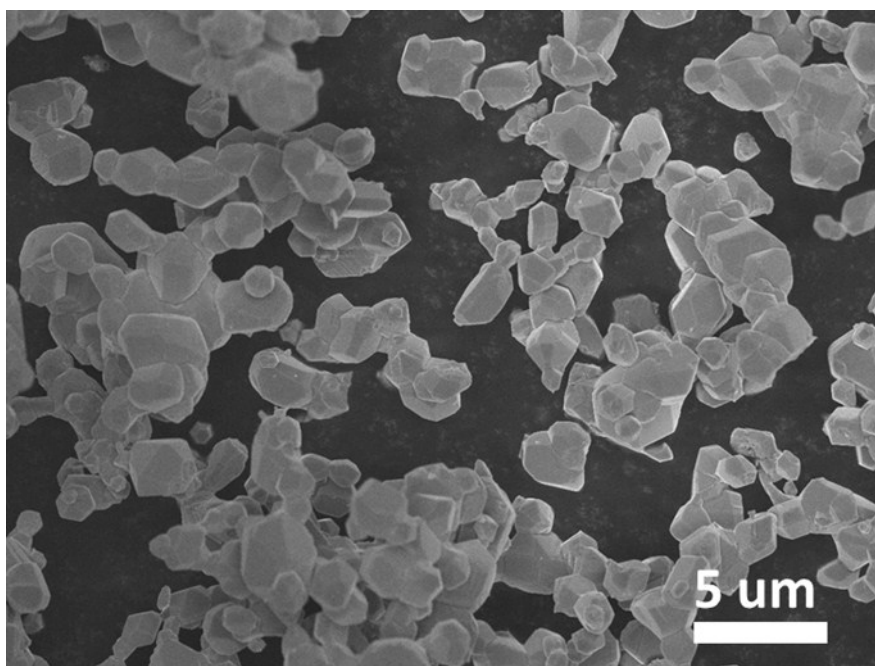


Fig. S4 SEM image of the pure $\text{CoS}_{1.097}$ nanoparticles.

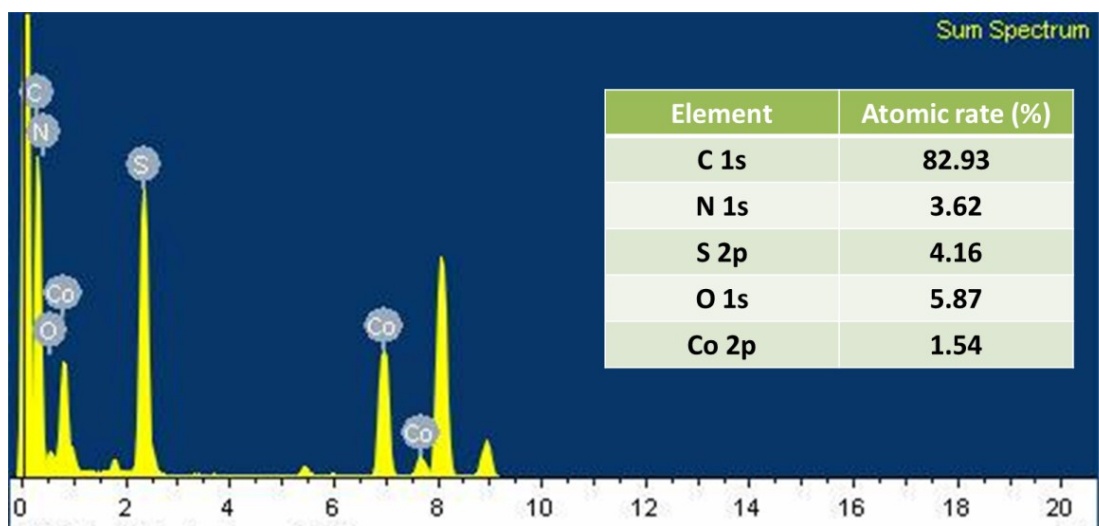


Fig. S5 Elemental contents and atomic rate in the $\text{CoS}_{1.097}/\text{GF}$ composite.

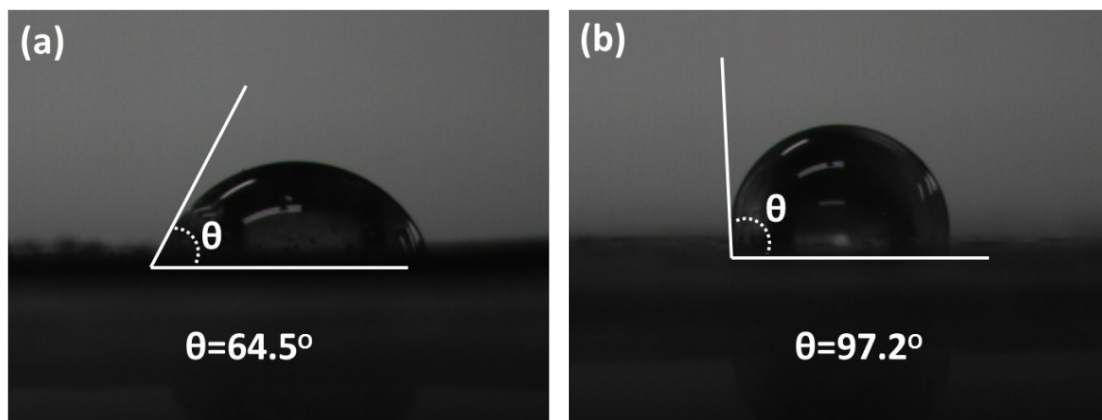


Fig. S6 The water contact angle measurement for a) $\text{CoS}_{1.097}/\text{GF}$ composite film, b) pure graphene film.

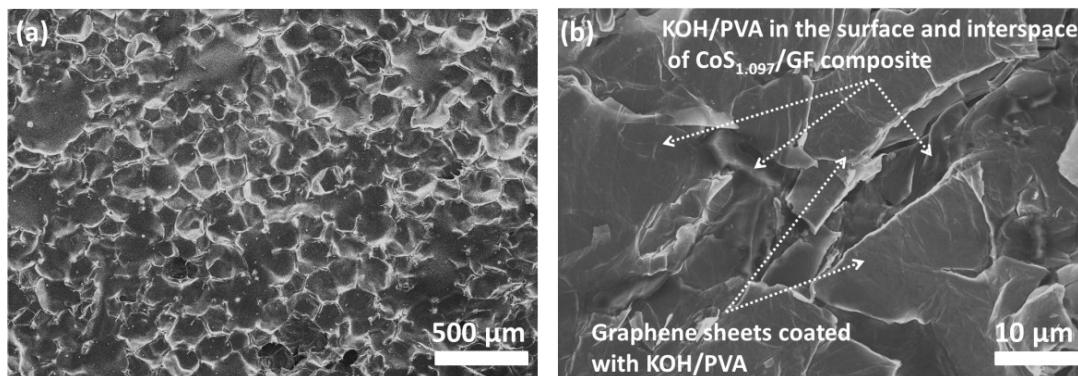


Fig. S7 SEM images of (a) the surface of porous $\text{CoS}_{1.097}/\text{GF}$ composite fulfilled with KOH/PVA electrolyte, (b) high magnification of porous $\text{CoS}_{1.097}/\text{GF}$ composite fulfilled with KOH/PVA electrolyte.

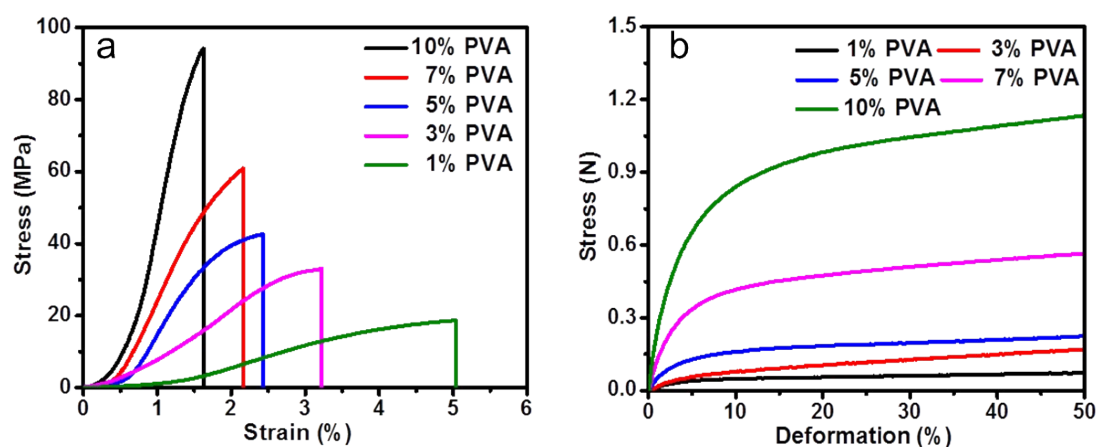


Fig. S8 (a) The stress-strain and (b) stress-deformation curves of $\text{CoS}_{1.097}/\text{GF}/\text{KOH}/\text{PVA}$ composite films with different PVA contents using the KOH/PVA as solid electrolyte.

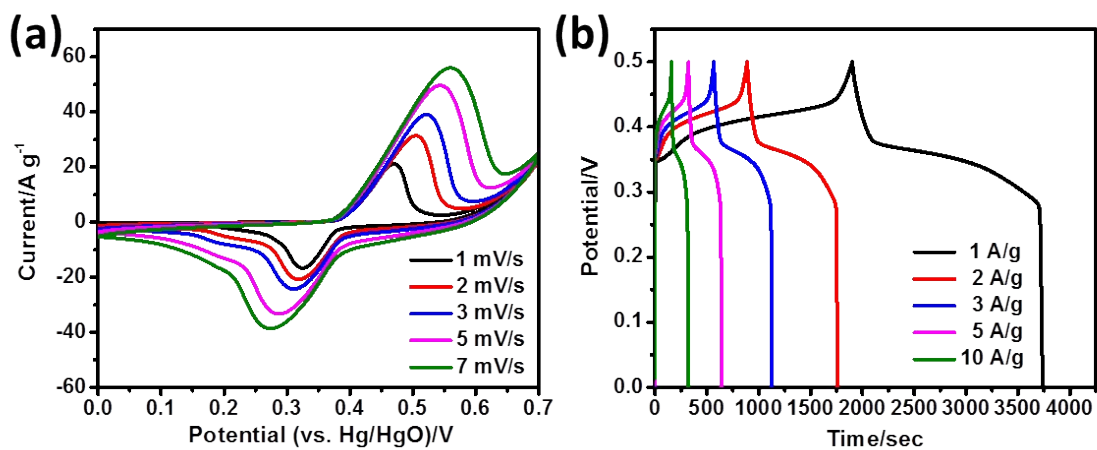


Fig. S9 (a-b) CV and GCD curves of CoS/GF-600 composite electrode.

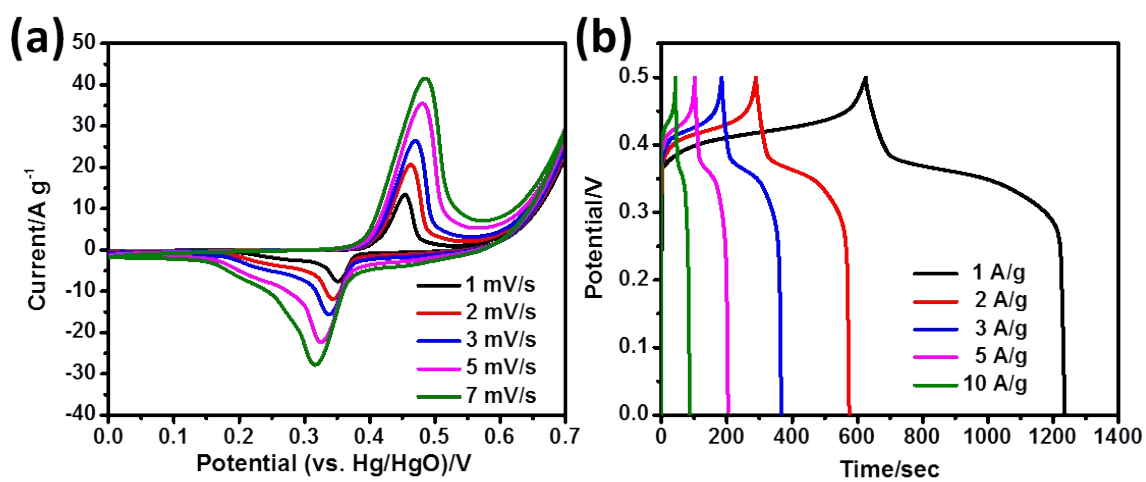


Fig. S10 (a-b) CV and GCD curves of CoS/GF-400 composite electrode.

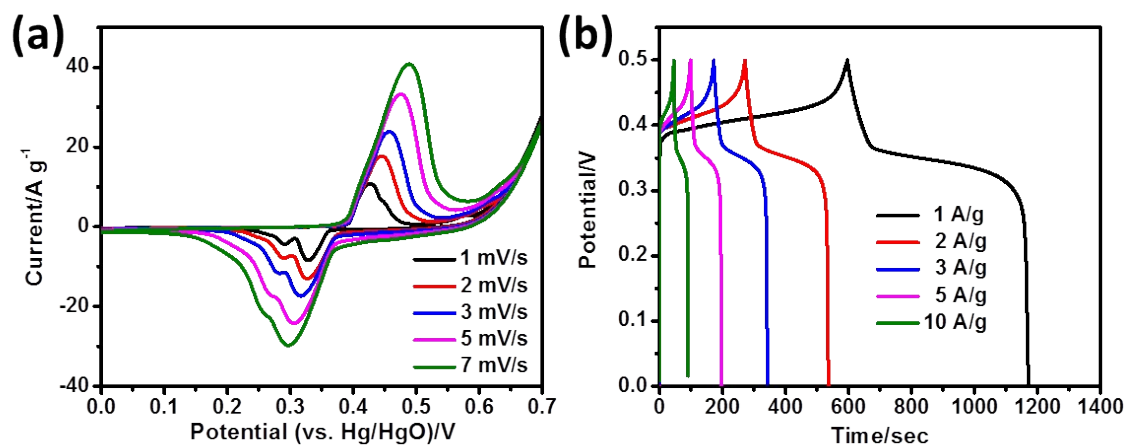


Fig. S11 (a-b) CV and GCD curves of CoS_{1.097}/GF-1:2 composite electrode.

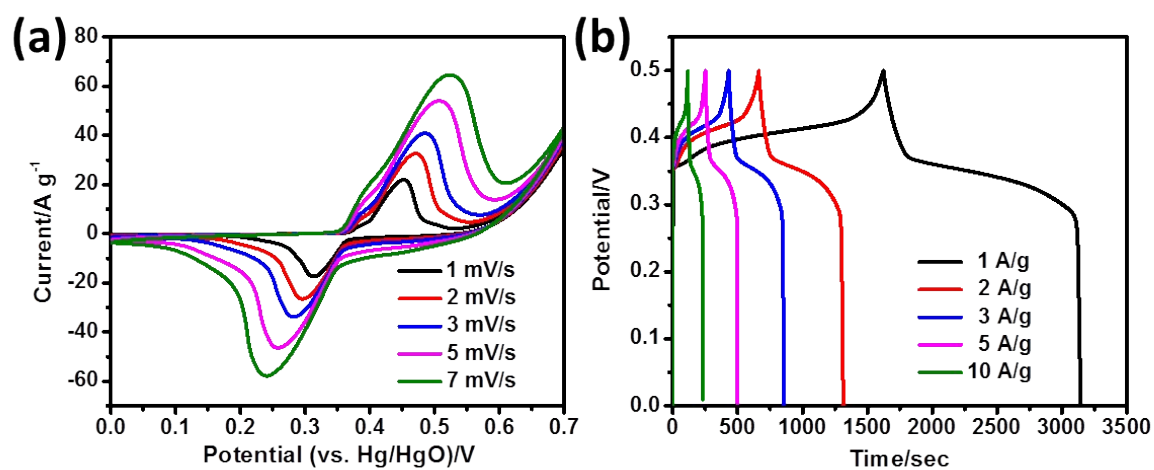


Fig. S12 (a-b) CV and GCD curves of CoS_{1.097}/GF-2:1 composite electrode.

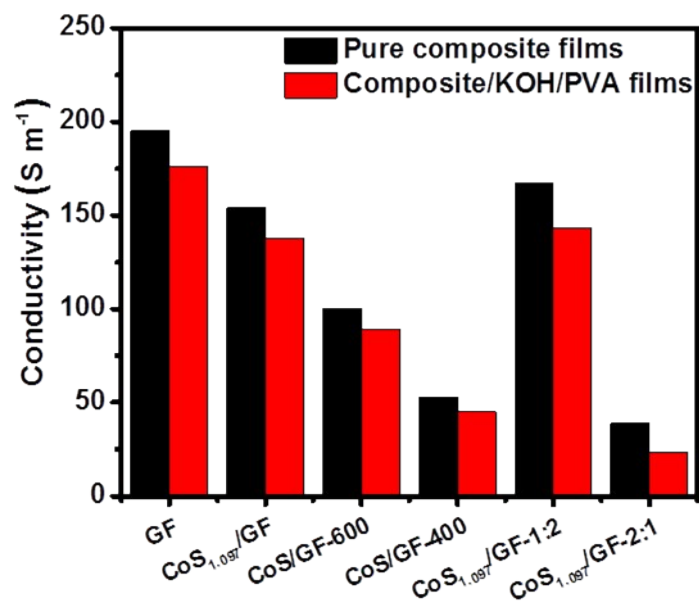


Fig. S13 (Black bar) the conductivity of the pure GF, CoS_{1.097}/GF, CoS/GF-600, CoS/GF-400, CoS_{1.097}/GF-1:2 and CoS_{1.097}/GF-2:1 composite film electrodes, respectively. (Red bar) the conductivity of the GF, CoS_{1.097}/GF, CoS/GF-600, CoS/GF-400, CoS_{1.097}/GF-1:2 and CoS_{1.097}/GF-2:1 composite fulfilled with KOH/PVA film electrodes, respectively.

Electrode material	Electrolyte	Current density (A g ⁻¹)	Specific capacitance (F g ⁻¹)	Ref.
CoS _{1.097} /GF	KOH (6 M)	1.0 A g ⁻¹	4475	This work
CoS/Graphene	KOH (2M)	1.0 A g ⁻¹	3785	1
CoS _{1.097} /N-doped Carbon	KOH (2M)	1.5 A g ⁻¹	360.1	2
CoS/Graphene	KOH (2M)	2.0 A g ⁻¹	1535	3
Ni ₃ S ₂ /CoNi ₂ S ₄	KOH (6M)	2.0 A g ⁻¹	2435	4
Ni-Co-S/Graphene	KOH (6M)	3.0 A g ⁻¹	1354	5
Co-Mn-HTS	KOH (2M)	2.0 A g ⁻¹	1093	6
NiCo ₂ O ₄ /NiWO ₄	KOH (6M)	1.0 A g ⁻¹	1384	7
NiCo ₂ O ₄ /MnO ₂	KOH (1M)	1.0 A g ⁻¹	913.6	8
NiCo ₂ O ₄ /PPy	KOH (3M)	1.0 A g ⁻¹	2244	9
Ni-Co-S	KOH (6M)	2.0 A g ⁻¹	1304	10

Table S1. Comparison of specific capacitance values of this work and those previously reported for metal sulfide/oxide electrodes.

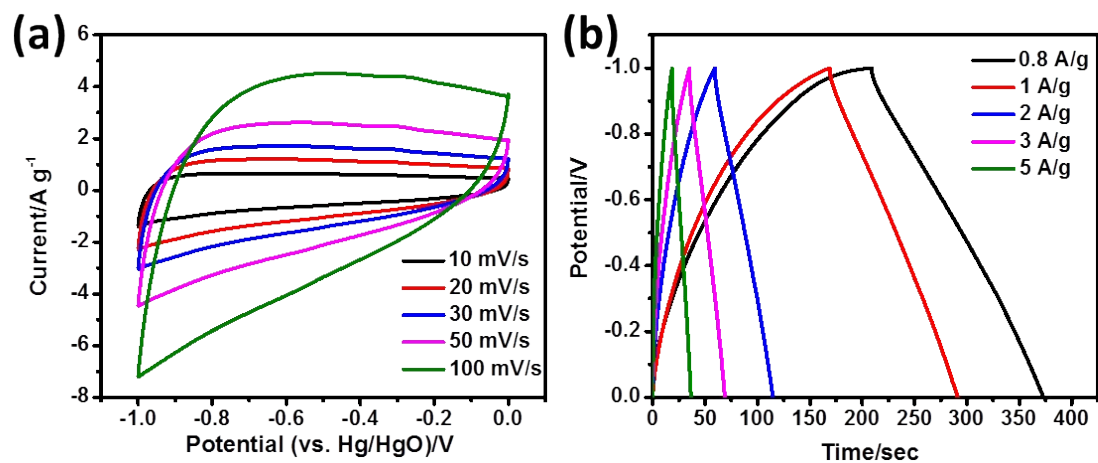


Fig. S14 (a-b) CV and GCD curves of GF electrode.

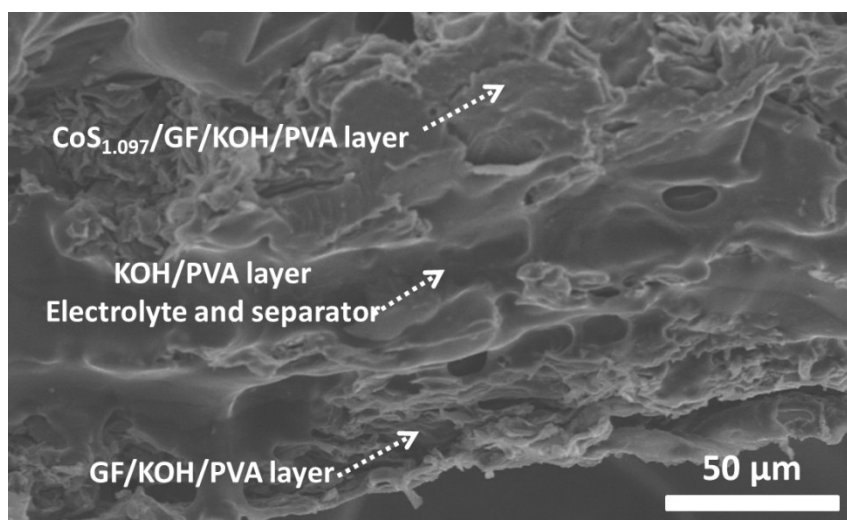


Fig. S15 SEM image of the cross section of the CoS_{1.097}/GF||GF a-EC film.

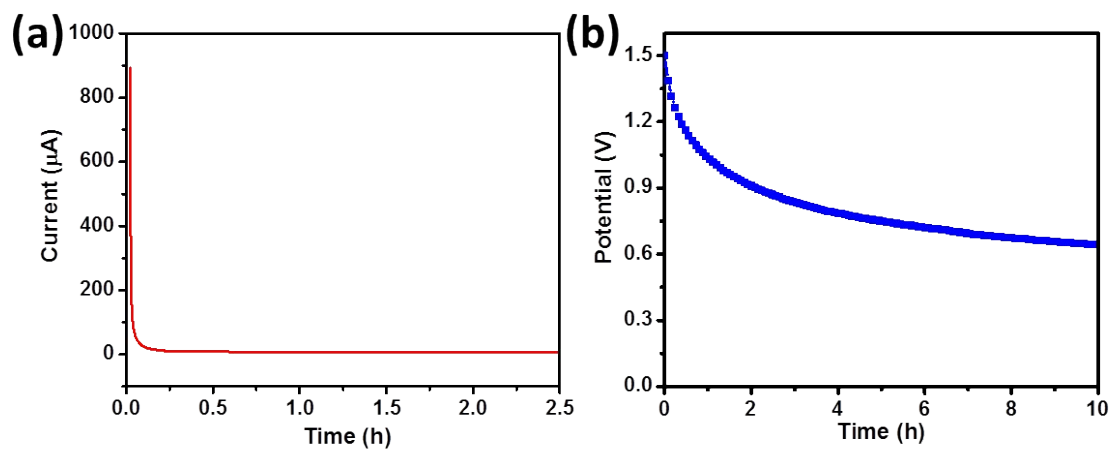


Fig. S16 (a) Leakage current and (b) self-discharge curves of the $\text{CoS}_{1.097}/\text{GF}||\text{GF}$ a-EC device against time.

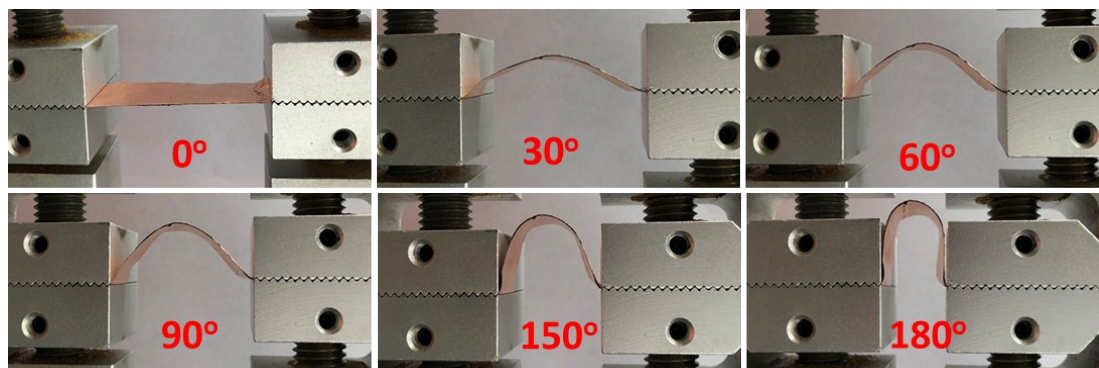


Fig. S17 The $\text{CoS}_{1.097}/\text{GF}||\text{GF}$ a-EC devices bended at different angles (0° , 30° , 60° , 90° , 150° and 180°).

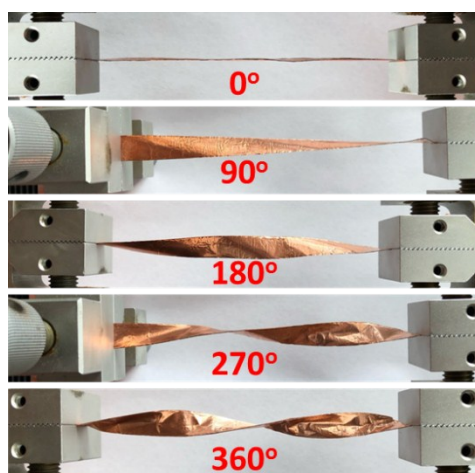


Fig. S18 The $\text{CoS}_{1.097}/\text{GF}||\text{GF}$ a-EC devices twisted at different angles (0° , 90° , 180° , 270° and 360°).

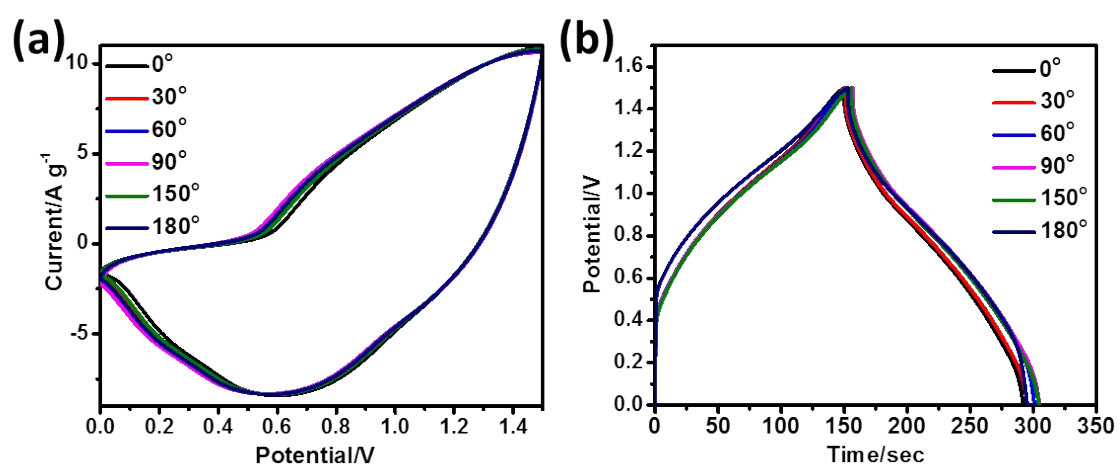


Fig. S19 (a-b) CV and GCD curves of the $\text{CoS}_{1.097}/\text{GF}||\text{GF}$ a-EC device measured at different bending angles (0° , 30° , 60° , 90° , 150° and 180°).

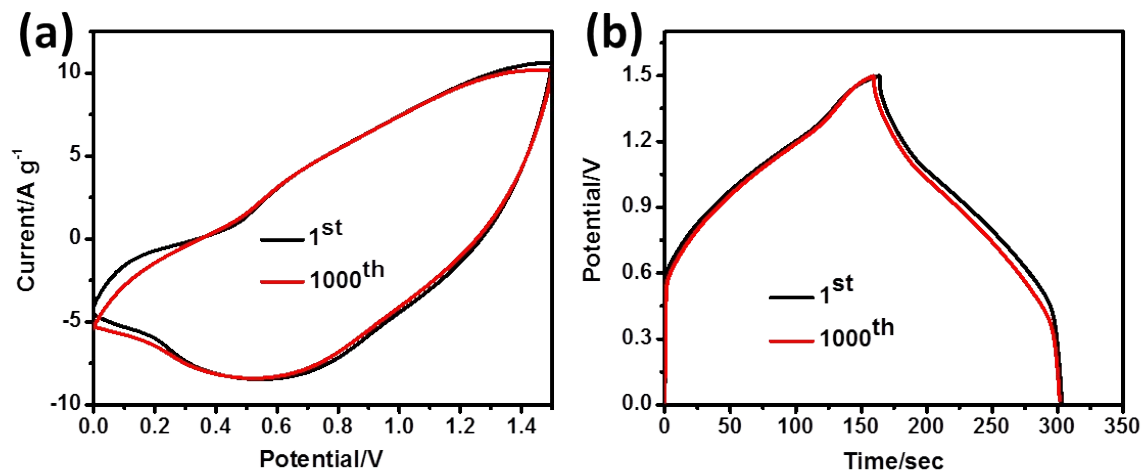


Fig. S20 (a-b) CV and GCD curves of the CoS_{1.097}/GF||GF a-EC device measured at initial and after 1000th bending tests.

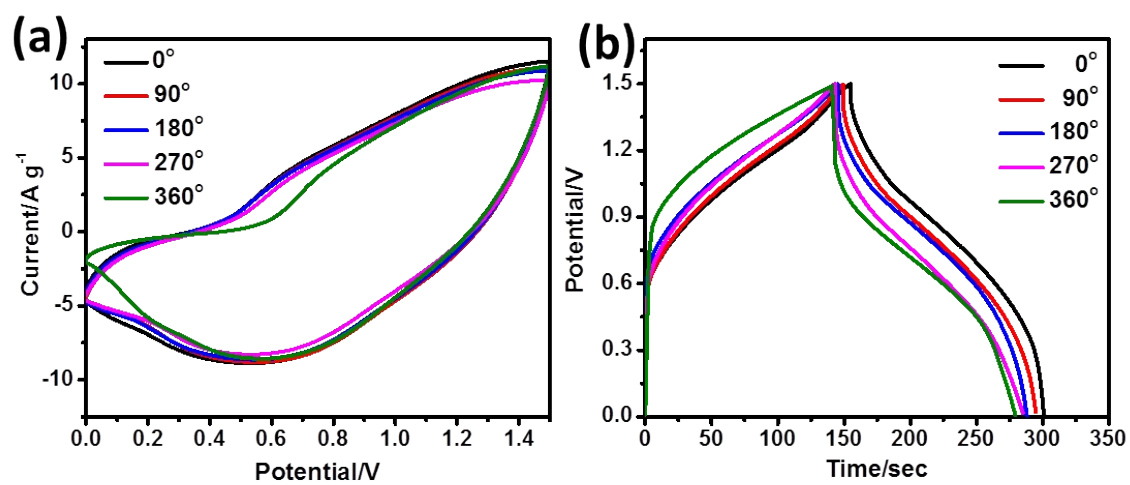


Fig. S21 (a-b) CV and GCD curves of the CoS_{1.097}/GF||GF a-EC device measured at different twist angles (0°, 90°, 180°, 270° and 360°).

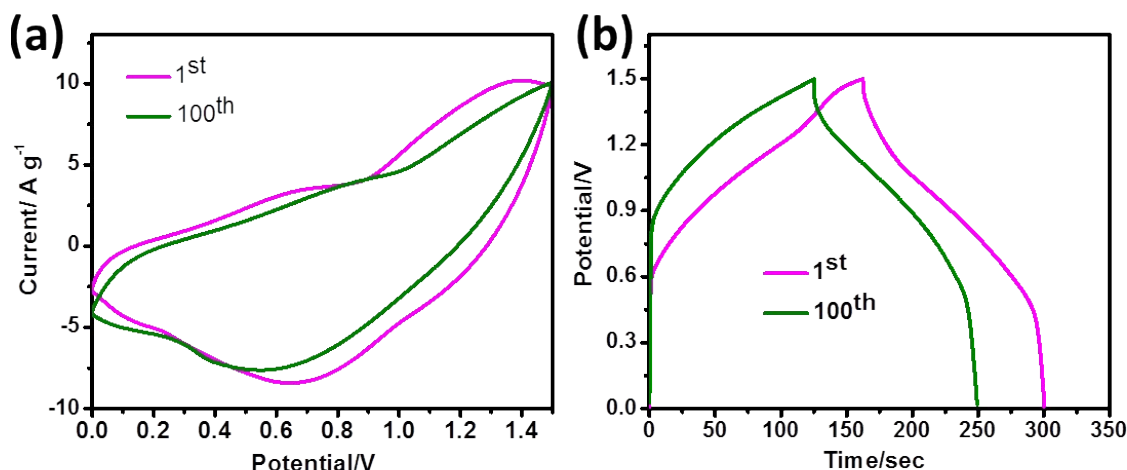


Fig. S22 (a-b) CV and GCD curves of the CoS_{1.097}/GF||GF a-EC device measured at the first and 100th twist tests.

Reference

1. J. H. Shi, X. C. Li, G. H. He, L. Zhang and M. Li, *J. Mater. Chem. A*, 2015, **3**, 20619-20626.
2. F. F. Cao, M. T. Zhao, Y. F. Yu, B. Chen, Y. Huang, J. Yang, X. H. Cao, Q. P. Lu, X. Zhang, Z. C. Zhang, C. L. Tan and H. Zhang, *J Am Chem Soc*, 2016, **138**, 6924-6927.
3. B. H. Qu, Y. J. Chen, M. Zhang, L. L. Hu, D. N. Lei, B. A. Lu, Q. H. Li, Y. G. Wang, L. B. Chen and T. H. Wang, *Nanoscale*, 2012, **4**, 7810-7816.
4. W. D. He, C. G. Wang, H. Q. Li, X. L. Deng, X. J. Xu and T. Y. Zhai, *Advanced Energy Materials*, 2017, **7**.
5. J. Yang, C. Yu, X. M. Fan, S. X. Liang, S. F. Li, H. W. Huang, Z. Ling, C. Hao and J. S. Qiu, *Energy Environ. Sci.*, 2016, **9**, 1299-1307.
6. Y. Guo, L. Yu, C. Y. Wang, Z. Lin and X. W. Lou, *Adv. Funct. Mater.*, 2015, **25**, 5184-5189.
7. S. M. Chen, G. Yang, Y. Jia and H. J. Zheng, *J. Mater. Chem. A*, 2017, **5**, 1028-1034.
8. Y. B. Zhang, B. Wang, F. Liu, J. P. Cheng, X. W. Zhang and L. Zhang, *Nano Energy*, 2016, **27**, 627-637.
9. D. Z. Kong, W. N. Ren, C. W. Cheng, Y. Wang, Z. X. Huang and H. Y. Yang, *Acs Applied Materials & Interfaces*, 2015, **7**, 21334-21346.
10. X. M. Li, Q. G. Li, Y. Wu, M. C. Rui and H. B. Zeng, *Acs Applied Materials & Interfaces*, 2015, **7**, 19316-19323.